Endophilin A1 induces different membrane shapes using a conformational switch that is regulated by phosphorylation

Mark R. Ambroso, Balachandra G. Hegde[1], and Ralf Langen[2]

Department of Biochemistry and Molecular Biology, Zilkha Neurogenetic Institute, Keck School of Medicine, University of Southern California, Los Angeles, CA 90033

Edited by Wayne L. Hubbell, University of California, Los Angeles, CA, and approved April 1, 2014 (received for review February 5, 2014)

Membrane remodeling is controlled by proteins that can promote the formation of highly curved spherical or cylindrical membranes. How a protein induces these different types of membrane curvature and how cells regulate this process is still unclear. Endophilin A1 is a protein involved in generating endocytotic necks and vesicles during synaptic endocytosis and can transform large vesicles into lipid tubes or small and highly curved vesicles in vitro. By using EM and electron paramagnetic resonance of endophilin A1, we find that tubes are formed by a close interaction with endophilin A1's BIN/amphiphysin/Rvs (BAR) domain and deep insertion of its amphipathic helices. In contrast, vesicles are predominantly stabilized by the shallow insertion of the amphipathic helical wedges with the BAR domain removed from the membrane. By showing that the mechanism of membrane curvature induction is different for vesiculation and tubulation, these data also explain why previous studies arrived at different conclusions with respect to the importance of scaffolding and wedging in the membrane curvature generation of BAR proteins. The Parkinson disease-associated kinase LRRK2 phosphorylates S75 of endophilin A1, a position located in the acyl chain region on tubes and the aqueous environment on vesicles. We find that the phosphomimetic mutation S75D favors vesicle formation by inhibiting this conformational switch, acting to regulate endophilin A1-mediated curvature. As endophilin A1 is part of a protein superfamily, we expect these mechanisms and their regulation by posttranslational modifications to be a general means for controlling different types of membrane curvature in a wide range of processes in vivo.

site-directed spin labeling | double electron–electron resonance

Numerous cellular remodeling events are controlled by proteins that can regulate membrane shape (1). In the example of synaptic endocytosis, proteins must engender invagination, drive pit formation, stabilize neck structures, and ultimately cause fission. These steps are executed through spatial and temporal application of membrane-altering proteins that contribute a range of curvatures (2, 3). Moreover, misregulated expression or posttranslational modification of these proteins is implicated in a number of diseases (4–7).

An increasing body of evidence suggests that endophilin plays an essential role in synaptic endocytosis by recruiting cofactors such as dynamin (8–10) and synaptojanin (11–14) as well as by inducing membrane curvature (15–18). It has been observed to localize to the synaptic vesicle pool and endocytotic neck regions in vivo and generate small highly curved vesicles and lipid tubes from large vesicles in vitro (8, 9, 11, 19). It has thus been proposed that a main component of the function of endophilin in vivo is its ability to regulate membrane curvature.

In general, proteins generate curvature through several mechanisms: by forcing membranes to conform to their own intrinsic protein shape (i.e., scaffolding) (3), inserting amphipathic segments into the lipid bilayer and thus generating a wedging force (20), protein crowding (21), and a less considered mechanism of space-filling whereby protein insertions alleviate packing differences between the inner and outer leaflet of the membrane (i.e., bilayer couple) (22). It is still unclear whether endophilin A1 uses a combination of mechanisms to generate the various types of membrane curvature or whether different mechanisms are used to cause vesiculation or tubulation.

The structure of endophilin A1 was first elucidated through crystallography and found to contain a crescent-shaped BIN/amphiphysin/Rvs (BAR) domain (17, 18, 23) [Fig. 1*A*; Protein Data Bank (PDB) ID code 2C08]. Mutational analyses of endophilin A1 have discovered that the loss of positively charged amino acids on the concave surface of the BAR domain inhibits the ability of endophilin A1 to curve lipid membranes (17, 24). The natural shape of the BAR domain implies that endophilin binds membranes and induces its intrinsic curvature through a scaffolding mechanism (25–27). Surprisingly, we found that, when bound to highly curved vesicles (similar in size to synaptic vesicles), the BAR domain of endophilin A1 resides at a significant distance from the membrane (28), where the scaffolding mechanism is not likely to be very strong. Instead, we found that the main contacts were made by the N-terminal (H0; residues 1–20) and insert region (residues 60–87) helices of endophilin A1, which are only partially resolved in the crystal structure (17, 28). These regions form amphipathic α-helices, which embed in the membrane at the level of the lipid phosphates. The locations of the helices are optimized for curvature sensing (29) and inducing (30, 31) through the wedging mechanism. In fact, helices alone can be sufficient to bend membranes, as shown by studies of α-synuclein (32, 33).

As of now, high-resolution structural data of endophilin bound to tubes has been limited. Studies that used cryo-EM in conjunction

Significance

BIN/amphiphysin/Rvs (BAR) proteins shape lipid membranes into functional shapes and compartments in a broad range of cellular processes. However, how a protein generates distinct forms of membrane curvature and how these states are regulated is unknown. We find that endophilin A1 uses different structures and mechanisms to generate tubes or vesicles. Phosphorylation toggles a conformational switch between these two structures, potentially acting as a regulator of membrane curvature in vivo. These findings may also explain how other proteins, including the BAR protein family, generate different shapes and are regulated in a large number of membrane remodeling processes.

Author contributions: M.R.A., B.G.H., and R.L. designed research; M.R.A. and B.G.H. performed research; M.R.A., B.G.H., and R.L. analyzed data; and M.R.A. and R.L. wrote the paper.

The authors declare no conflict of interest.

This article is a PNAS Direct Submission.

[1]Present address: Post Graduate Department of Physics, Rani Channamma University, Vidyasangama, Belagavi 591156, Karnataka, India.

[2]To whom correspondence should be addressed. E-mail: Langen@usc.edu.

This article contains supporting information online at www.pnas.org/lookup/suppl/doi:10.1073/pnas.1402233111/-/DCSupplemental.

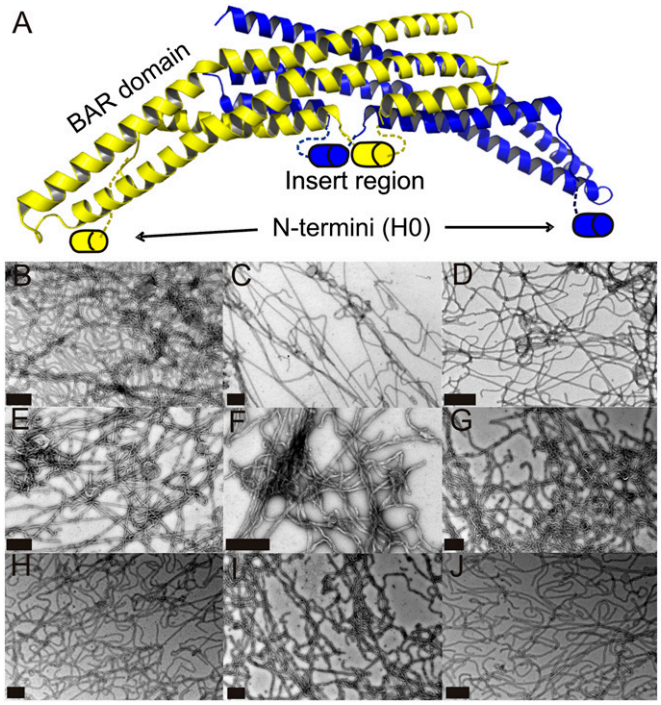

Fig. 1. Endophilin A1-induced tubulation. (*A*) The crystal structure of rat endophilin A1 (PDB ID code 2C08) dimer (subunits are colored yellow or blue). The N-termini (H0) and insert region are schematically illustrated as cylinders to indicate their ability to become helical upon membrane binding (17, 28, 35). Lipid tubes generated from large vesicles incubated with spin-labeled (R1) endophilin A1 derivatives are visualized by negative stain transmission EM. Representative examples are shown for N-terminal derivatives 5R1 (*B*), 6R1 (*C*), and 13R1 (*D*); insert region derivatives 70R1 (*E*), 71R1 (*F*), and 77R1 (*G*); and BAR domain derivatives 108R1 (*H*), 159R1 (*I*), and 247R1 (*J*). All samples were screened for thorough tubulation before further experimentation. (Scale bars: 500 nm.)

with computational modeling have shown that BAR domains take up specific high-density oligomeric states that appear to stabilize tube structures by acting as scaffolds (34–36). However, scaffolding would likely be ineffective if tube-bound endophilin had the same remote membrane binding as observed on vesicles. For these reasons, the main goal of the present study was to investigate whether endophilin A1 uses different structures and mechanisms in generating tubes than in forming vesicles. We hypothesize that defining these two states will provide insight into not only how one protein can generate multiple types of membrane curvature but how they might be regulated in the cell.

We find that, in comparison with the structure on liposomes (17, 28), tube-bound endophilin shifts the concave surface of its BAR domain close to the membrane, and the H0 and insert regions, concertedly, submerge below the lipid phosphates and into the acyl chains. These data suggest a more pronounced role of scaffolding. The concerted downward movement of the helices appears to be important for tubulation. We noticed that S75, a phosphorylation site targeted by Parkinson disease (PD)-associated LRRK2 kinase (4), is shallowly inserted on vesicles but deeply on tubes. We hypothesized that the introduction of a negative charge would create a large energetic cost for deeply inserting S75 in the tube conformation. In fact, we found phosphomimetic mutation S75D to destabilize tubulation through favoring shallow insertion of the insert helices and not by a decrease in membrane association. It is possible that LRRK2-mediated phosphorylation of S75 could act as an important regulator for how endophilin structurally interacts with and curves membranes. As mutations that constitutively activate LRRK2 represent the most common form of inherited PD, determining how phosphorylation alters the structure and function of endophilin A1 is of significant importance.

Results

On Tubes, N-Terminal α-Helices Insert Deeply into the Acyl Chain Region of the Lipid Membrane. To investigate the structure of tube-bound endophilin A1, we first optimized conditions for tubulation. According to transmission EM (Fig. 1 *B–J*), we were able to generate homogeneous tubes with an average diameter of 35 nm and a typical length of 10 μm that were stable for at least 24 h. Then, we used these conditions in site-directed spin labeling studies aimed at determining the local structure and location of the H0 when endophilin A1 is bound to tubes. Endophilin A1 was spin labeled at select sites in its H0, one at a time, and these derivatives were confirmed to tubulate vesicles under optimized conditions. Continuous-wave (CW) electron paramagnetic resonance (EPR) spectra of these spin-labeled positions (R1 denotes presence of a spin label) indicate an ordering of the H0 upon tube formation (Fig. 2*A*). Thus, H0, which is unfolded in solution, becomes structured on lipid tubes. A spin label's depth in the lipid bilayer can be detected by using a collision-gradient method, which measures the relative accessibility of the label to lipophilic oxygen and lipophobic NiEDDA (37). To determine the immersion depth of H0 in a tube-bound state, we measured the accessibility of the spin-labeled derivatives to O_2 (ΠO_2) and NiEDDA (ΠNiEDDA) and calculated the depth parameter Φ [$\Phi = \ln(\Pi O_2/\Pi NiEDDA]$ (37). Increasing depth of a spin label in the lipid bilayer will cause exposure to high levels of oxygen and minimal levels of NiEDDA, resulting in an increased Φ value, and alternatively, solvent-exposed spin labels will give low to negative Φ values. Positive Φ values were observed for sites on the hydrophobic face, and low to negative Φ values were observed for the sites on the hydrophilic face of the H0 helices (Fig. 2*B*). After calibration (Fig. S1), we converted Φ values into depth and found that labeled sites lining the hydrophobic face of the H0 helices penetrate deeper into tubes than into vesicles (Fig. 2*C*). The average immersion depth of these sites was 18 Å. Inasmuch as the nitroxide moiety is typically 7–10 Å from the center of the helix (38), we can estimate that the depth of the H0 helix is on the order of 8–11 Å below the lipid phosphates (Fig. 2*D*).

The H0 region was previously shown to be necessary for stable oligomerization of endophilin on tubes, and cross-linking data suggested that this could be mediated by an interaction between neighboring H0 from different dimers (35). To examine whether this stabilization was mediated by a direct contact between neighboring H0 helices, residues lining either side of the amphipathic H0 helix were selected and examined for the presence of spin-coupling while bound to tubes (Fig. 2*E*). No presence of spin-coupling or line-shape changes upon dilution of these spin labeled mutants with cysless analogs was observed, suggesting that the labeled sites on the helices do not stably reside within 20 Å of each other. We therefore used double electron-electron resonance (DEER), which has a significantly longer range (as much as 60–70 Å). Intermolecular distances were measured by using endophilin labeled at position 7 or 12, which are close to the center of the H0 helix. We found broad distance distributions with peaks around 30–40 Å, suggesting that neighboring H0 helices may not have one unique orientation to each other and are unlikely to be in direct contact (Fig. 2 *F* and *G*).

On Tubes, Insert Region Inserts Deeply into Acyl Chain Region, and BAR Domain Contacts the Lipid Headgroups. Next, we investigated whether endophilin A1 regions other than H0 differently interact with tubes and vesicles. Our prior studies on vesicle-bound endophilin A1 revealed that residues 63–75 of the insert region take up an α-helical conformation (28). In the dimer, these helices are antiparallel to one another and largely perpendicular to the long axis of the BAR domain (Fig. 1*A*). Thus, we first

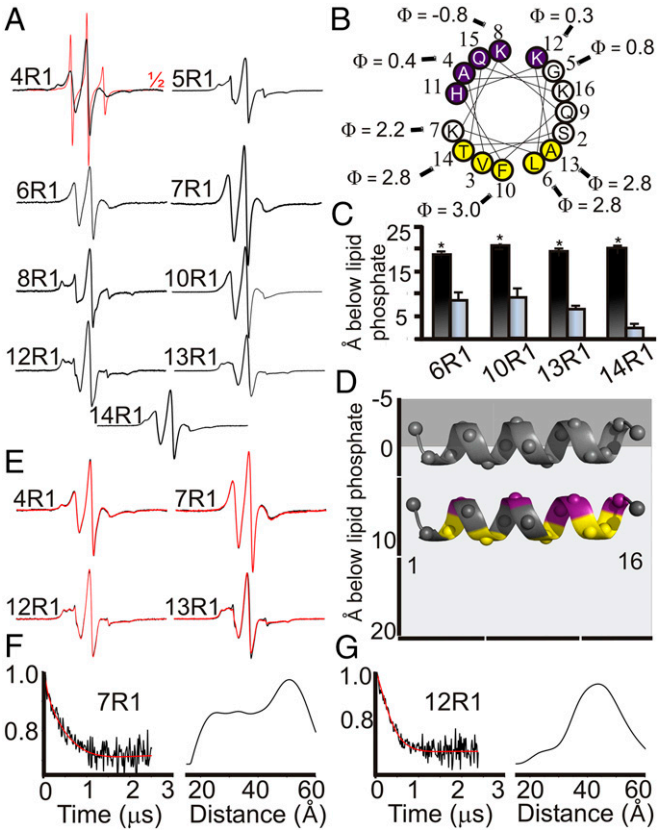

Fig. 2. N-terminal helices penetrate deeply into the membrane. (*A*) CW EPR spectra of spin-labeled (R1) endophilin A1 derivatives bound to tubes (black). The EPR spectrum of position 4 in solution (red) is representative of other N-terminal sites and is shown at half amplitude. (*B*) Helical wheel depiction of H0 showing a hydrophilic (purple) and hydrophobic (yellow) face. Measured Φ values are shown for select residues. (*C*) Φ Values were converted into immersion depths for sites on the hydrophobic face of H0 on tubes (black) or in a previously elucidated vesicle-bound (gray) state (17). Depths represent the location of the nitroxide label which is typically 7–10 Å from the center of the α-helix (38). (*D*) A schematic model of the H0 helices on small vesicles (gray helix) or tubes (colored helix as in *B*) relative to the lipid headgroups (gray) and acyl chains (light gray). The helices were manually placed according to the observed average immersion depth of lipid-exposed sites, taking into account the length of the nitroxide side chain. (*E*) CW EPR spectra of select endophilin A1 derivatives on tubes fully labeled (black) or mixed with threefold excess of unlabeled protein (red). The overlay of the respective spectra indicates the absence of significant spin–spin interactions. (*F* and *G*) Baseline subtracted time-evolution data (black, *Left*) from DEER experiments of the indicated tube-bound endophilin derivatives were subjected to Tikhonov regularization (red), resulting in the shown distance distributions (*Right*). Error bars represent SD; $n = 3$ independent experiments (*$P < 0.005$, Student t test).

investigated whether the insert helices retain this orientation upon tubulation. DEER distances between singly labeled mutants in the insert region were similar, albeit slightly longer than those previously reported for vesicle-bound protein (Fig. 3 *A*–*C* and Fig. S2*A*). Thus, the antiparallel and α-helical structure is retained under tubulating conditions. Moreover, CW EPR spectra of spin labeled mutants 63–79 showed signs of ordering comparable to that seen for the same region bound to vesicles (Fig. S2 *B* and *C*). To determine whether the insert helices immerse themselves more deeply into the bilayer of tubes, accessibility-based depth measurements were performed by replacing each side chain with R1 one amino acid at a time. The Φ values display a periodicity indicative of an α-helix and fit well onto a helical wheel; high Φ values fall onto one surface (hydrophobic face; Fig. 3 *D* and *E*, yellow) and low Φ values onto the opposite surface (hydrophilic face; Fig. 3 *D* and *E*, purple). After calibration, the depth of the spin labeled sites suggest a helical axis 5–8 Å deep in the membrane (Fig. 3*F*). Residues 76–79 retain a periodicity consistent with an α-helical structure, but the variation in depth is no longer as pronounced (Fig. S3). These residues are likely to be in a transition region

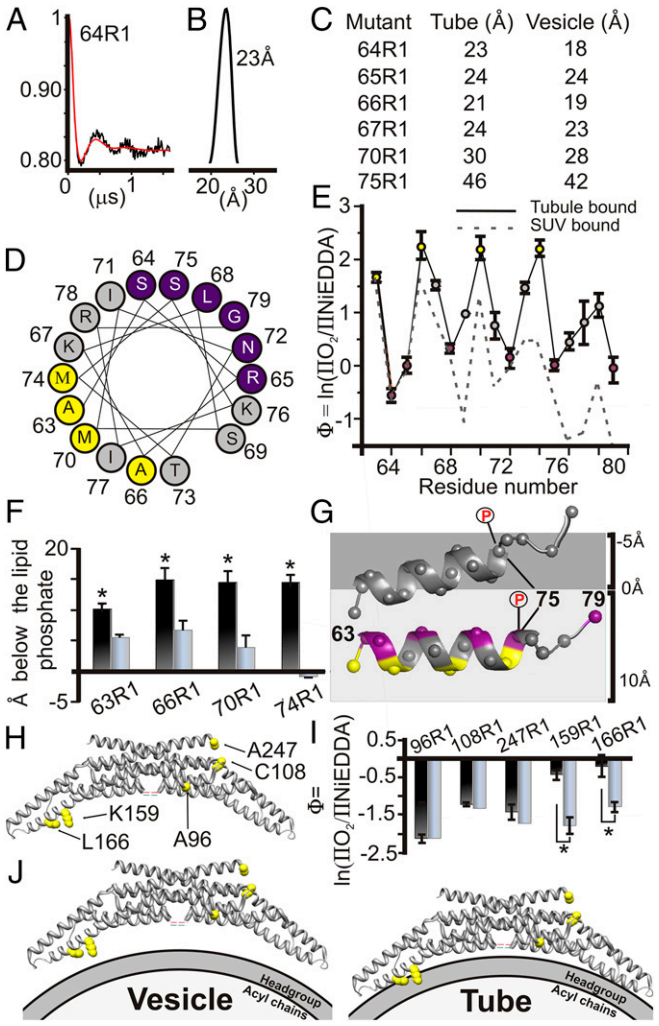

Fig. 3. Concerted movement of BAR domain and insert region toward the membrane. (*A*) Baseline subtracted time-evolution data (black) from a DEER experiment of tube-bound 64R1 subjected to Tikhonov regularization (red) with (*B*) resulting distance distribution. (*C*) A comparison between intradimer distances on vesicles (28) and on tubes. (*D*) Local Φ maxima (yellow) and minima (purple) fall onto a hydrophobic or hydrophilic face of a helical wheel. (*E*) Φ as function of labeling position on tubes (solid, colored as in *D*) and on vesicles (28) (dashed). (*F*) Immersion depth after calibration for sites on the hydrophobic face of the insert region on vesicles (28) (gray) and on tubes (black). (*G*) A schematic model of the insert region on vesicles (gray helix) and tubes (colored as in *D*) relative to the lipid headgroups (dark gray, negative depth values) and the acyl chains (light gray, positive depth values). The helices were manually placed as described in Fig. 2. The phosphorylation site S75 moves from the acyl chain environment to the aqueous environment (illustrated phosphate groups). (*H*) Crystal structure of rat endophilin A1 dimer (PDB ID code 2C08) showing the locations of spin-labeled sites. (*I*) Bar graph comparing Φ values measured for sites on the concave and convex surfaces of the BAR domain when bound to tubes (black) or vesicles (gray). (*J*) Schematic illustration of the location of the BAR domain relative to the bilayer when bound to vesicles (*Left*) or tubes (*Right*). Error bars represent SD; n represents at least three independent experiments (*$P < 0.01$, Student t test).

between a fully helical and a loop structure and may represent an additional helix-like structure not present on vesicles. The constant immersion depth of the membrane facing residues also indicates that the insert helices are parallel to the membrane and not upward-tilted as on vesicles (Fig. 3*G*).

Having established that the insert regions as well as the H0 helices move deeper into the bilayer, we wanted to investigate whether the BAR domain might also undergo similar movements. According to the crystal structure, residues 63–67 of the insert region are directly adjoined to the BAR domain, suggesting that the movement of the insert helices might be directly coupled to that of the BAR domain. To test this notion, spin-labeled sites previously used for vesicle-bound endophilin (28) were subjected to accessibility measurements (Fig. 3 *H* and *I*). On tubes, spin-labeled residues located on the concave surface, 159 and 166, showed increased Φ values, whereas all sites on the convex surfaces retained highly negative Φ values; these lie outside our depth calibration, and are therefore compared by Φ. However, spin labeled residues 159 and 166 lie inside our calibration range with values located ∼4–6 Å greater than the level of the lipid phosphates. Thus, tubulation causes a concerted movement of the BAR domain together with the H0 and insert region toward the membrane (Fig. 3*J*).

Phosphomimetic Mutation S75D Destabilizes Tubes by Preventing Deep Insertion of the Insert Helix. It is still unclear how endophilin A1 transitions between tubulation and vesiculation in vivo. A recent report elucidated a direct link between mutations in LRRK2 kinase and the increased phosphorylation of endophilin A1 at position S75 (4). Our structural data show that this position is located in a region that takes up a very different location with respect to the membrane when on tubes or vesicles (Fig. 3*G*). Although the S75 side chain was determined to reach above the lipid headgroups and into the aqueous environment on vesicles (28), it is deeply embedded in the acyl chain region upon tubulation. Given that the S75 side chain faces straight out of the membrane and approximating a phosphoserine side chain to be 4 Å long, one could estimate the negative charge to be around the lipid phosphates on tubes but well above the lipid headgroups on vesicles. We therefore hypothesized that S75 phosphorylation might preferentially destabilize the tube-bound conformation and favor the vesicle-bound structure. To test this, we first aimed to verify whether phosphorylation affects the overall membrane association of endophilin in vitro. By using a phosphomimetic mutation S75D in combination with spin-labeled derivative 74R1, we titrated S75-74R1 and S75D-74R1 with lipid vesicles (Fig. 4 *A* and *B*) and monitored binding via amplitude changes in EPR CW spectra (Fig. 4*C*). No difference in binding saturation was observed by using our optimized lipid composition, although a noticeable albeit small ($P > 0.1$) decrease was observed for binding to a previously used lipid system (4). To determine whether the phosphomimetic mutation affects the structure of endophilin A1, tube-bound S75D-74R1 and S75D-63R1 mutants were investigated by CW EPR. These labeled positions were selected to measure positions near both ends of the helix. Moreover, spin–spin interactions in the spectra of 63R1 are a useful determinant of endophilin dimerization (28). In comparison with their respective S75 counterparts, S75D-63R1 and S75D-74R1 had comparable CW EPR spectra but significantly reduced Φ values (Fig. 4 *D* and *E*). These data suggest that the mutants remain dimerized, membrane-associated, and in a similar local structure but at decreased depths within the bilayer. We then investigated whether the modification could affect the ability of endophilin to form tubes in our optimized tubulation system. Although the spin-labeled derivatives containing S75 (WT) produced tubes that were stable for days to weeks, S75D-63R1 and S75D-74R1 generated more vesiculation (Fig. 4 *F*–*I*). Similarly, comparison of unlabeled WT and S75D endophilin A1 constructs revealed that phosphomimetic mutants produce tubes initially but with decreased stability over a 24-h period and increased amounts of small vesicles (Fig. 4 *J* and *K*). In summary, the phosphomimetic modification at position S75 inhibits stable tubulation by shifting the insert region to shallower depths within the lipid bilayer.

Discussion

Compared with its vesicle-bound form (17, 28), different regions of tube-bound endophilin undergo a concerted structural reorganization that brings the BAR domain closer to the membrane and inserts the amphipathic helices more deeply into the acyl chain region. This orientation appears to be important as the introduction of a phosphomimetic negative charge at residue 75 destabilizes the more deeply embedded tube-bound structure in favor of other mainly vesicular forms, potentially representing

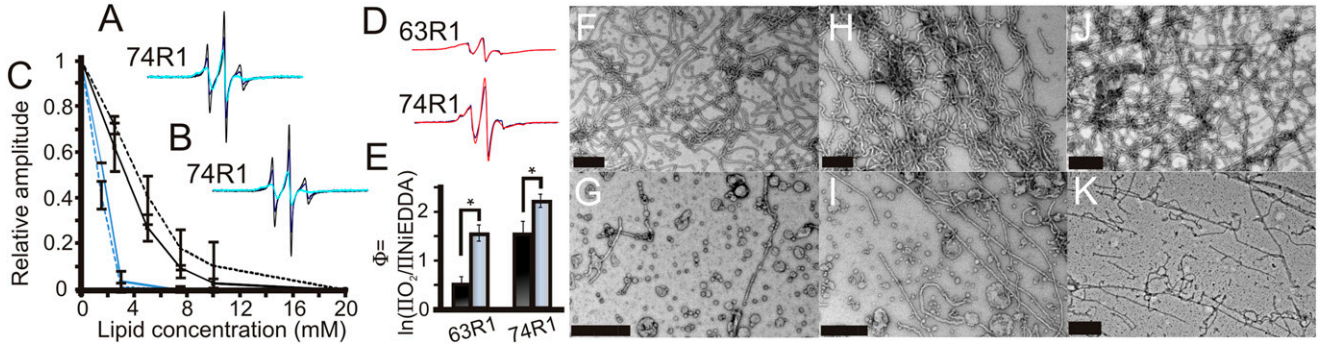

Fig. 4. Phosphomimetic S75D mutation destabilizes tubes by reducing membrane immersion depth of the insert region. CW EPR spectra of S75D-74R1 incubated with 0 mM (black), 2.5 mM (purple), and 10 mM (teal) of (*A*) vesicles composed of a 5:2:1:1 molar ratio of L-α-phosphatidylcholine, L-α-phosphatidylethanolamine, L-α-phosphatidylserine, and cholesterol (4) or (*B*) vesicles composed of 2-Dioleoyl-sn-Glycero-3-[Phospho-*rac*-(1-glycerol)] sodium salt and 1,2-Dioleoyl-sn-glycero-3-phosphoethanolamine (2:1). (*C*) Spectral amplitudes for S75-74R1 (solid lines) and S75D-74R1 (dashed lines) from the experiments in *A* (black lines) or *B* (blue lines) are plotted as function of lipid concentration. (*D*) CW EPR spectra of tube-bound endophilin A1 labeled at positions 63 or 74 with (black) or without (red) the S75D mutation. All spectra are normalized to the same number of spins. (*E*) Φ Values of 63R1 and 74R1 with (black) and without (gray) the S75D mutation incubated with 2-Dioleoyl-sn-Glycero-3-[Phospho-*rac*-(1-glycerol)] sodium salt and 1,2-Dioleoyl-sn-glycero-3-phosphoethanolamine (2:1). Negative stain EM shows S75-63R1 forming stable tubes after 24 h (*F*), whereas S75D-63R1 produces mainly vesicular structures (*G*). Similar results were obtained for S75-74R1 (*H*) and S75D-74R1 (*I*) as well as S75 (*J*) and S75D (*K*) in a WT background. (Scale bars: 0.5 μm.) Error bars represent SD; *n* represents at least three independent experiments (*$P < 0.005$, Student *t* test).

a regulatory mechanism responsible for guiding endophilin A1's curvature state.

The closer membrane proximity and direct contact of the BAR domain on tubes suggests a much more pronounced scaffolding effect. These present data, together with our previous study on vesicle-bound endophilin A1, suggests that there are two very different mechanisms by which vesicles or tubes are generated (Fig. 5 *A* and *B*). Although the membrane curvature of vesicles is predominantly stabilized by the insertion of endophilin's helical wedges, tubes are stabilized through a combination of scaffolding and helix insertion. Whereas the present study revealed two structural states, previous studies on endophilin A1 and the related amphiphysin identified two distinct functional modes of membrane interaction (39, 40). Under high protein density conditions, both N-BAR proteins behaved as potent inducers of membrane curvature and generated tubes similar in size to those observed here. In contrast, low protein density conditions had a smaller effect on membrane curvature induction. In agreement with cryo-EM data (34, 35), which showed a highly oligomeric protein coat around lipid tubes, it was suggested that increasing protein concentrations promoted the assembly of the protein scaffold (39, 40). The differential modes of membrane binding

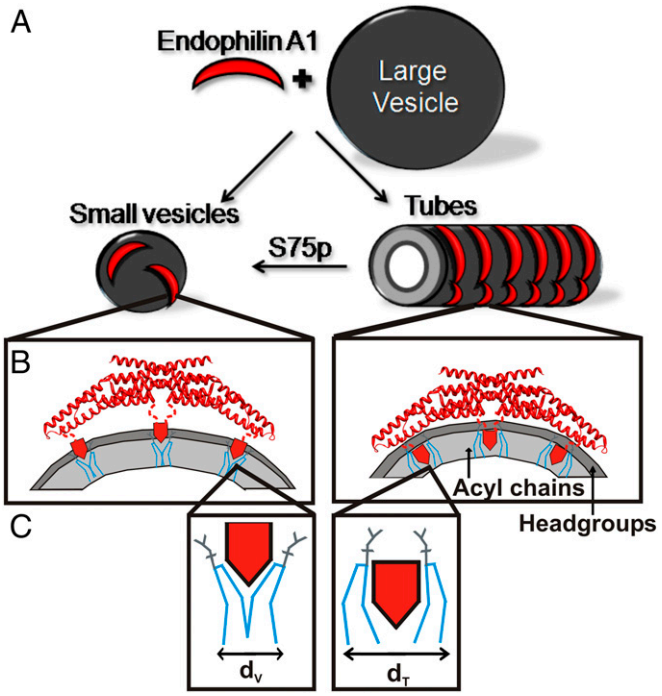

Fig. 5. Schematic illustration of endophilin A1 tube and vesicle binding and its modulation by phosphorylation. (*A*) The incubation of endophilin A1 and large lipid vesicles can result in vesiculation or tubulation. (*B*) On small vesicles (*Left*), endophilin A1 predominantly uses its amphipathic helices (red pentagons) rather than the BAR domain for membrane binding. The location of the helices is optimized for stabilizing membrane curvature by wedging into the headgroup region (dark gray) and thereby generating a splitting force between neighboring lipids (*C*, blue lines). Endophilin A1 binds tubes (*A*, *Right*) in a highly oligomeric, anisotropic manner (34, 35), and moves its amphipathic helices deeper into the acyl chains (*B*, *Right*), filling more space within the acyl chain region (light gray), which more optimally pushes entire lipids apart (*C*, *Right*). The difference in lipid area the helices take up in the membrane is greater for tubes (d_t) than for vesicles (d_v). Simultaneously, the BAR domain moves into contact with the lipid headgroups (*B*, *Right*). For simplicity only the outer leaflet of the membrane is shown in *B*. LRRK2 phosphorylation introduces a negative charge at S75, a site submerged in the acyl chain region of tubes. This modification destabilizes tubes and favors vesicles as illustrated in *A*.

are consistent with the observed structural rearrangements in tube-bound endophilin, which, as we find, do not only polymerize the BAR domains but also bring them closer to the membrane. Another recent study investigated the binding of endophilin and amphiphysin to intact vesicles of varying diameters. Interestingly, the curvature sensitivity solely relied on the amphipathic helices and not the BAR domain (29). This result would have been difficult to rationalize with a model in which the BAR domain is in close contact with the membrane. Rather, this finding is consistent with a model in which the BAR domain moves close to the membrane only when it engages in scaffolding and oligomerizing on tubes.

Although it is clear that the H0 helices play a critical role in oligomerization (35), the underlying mechanisms are still unknown. Our data are inconsistent with a model in which neighboring helices are directly aligned and in physical contact with each other. However, we cannot exclude models in which the neighboring helices are severely staggered or in which helices jointly coordinate a lipid bridge between them. The latter may be more likely because the sides of the helices are lined with positive charges. This would cause repulsion in the case of direct interaction between the helices but would favor association with negatively charged lipids.

Considering the shallow immersion depth typically observed by EPR for most membrane-bound amphipathic helices (20, 28, 32, 41, 42), it was surprising to discover the deeply inserted amphipathic helices on tubes. This movement brings the C_α of lysine residues deep into the acyl chain region (~7–10 Å). Although the membrane environment is an unfavorable location for lysines, it is likely that such side chains "snorkel" (43) to form a salt bridge with lipid phosphates. Given that an extended lysine side chain is 6.5 Å long and amine–phosphate bonds are ~3 Å, the submerged lysines are within range to snorkel to the lipid phosphates. This interaction could be facilitated further by a movement of the phosphate toward the lysine side chain. The deeper insertion of helical wedges is also likely to have some functional consequences. The downward movement of the helices reduces their ability to push the headgroups apart, thereby decreasing the spontaneous curvature effects (44) (Fig. 5*C*). A prior study, which combined mutagenesis and computational methods, found that strong spontaneous curvature contributions of helical wedges at high densities promoted vesiculation whereas enhanced scaffolding favored tubulation (45). According to this notion, the reduced spontaneous curvature of more deeply inserted helices may therefore be beneficial to tube stability and reduce vesiculation.

In addition, the increased helix immersion depths on tubes also promote acyl chain separation (Fig. 5*C*). By taking up additional space in the outer leaflet, the helices may compensate for the increasing imbalance between the surface areas of the inner and outer leaflet during tubulation. Such a bilayer couple-like mechanism could be especially important in membranes of low cholesterol in which there is little "flip-flop" (30). Interestingly, vesicle fusion events result in transleaflet flip-flop (46, 47). If similar lipid redistribution occurs during the reverse vesiculation process, the need for space filling may not be as important. Regardless of the exact reasons, our study on S75 phosphorylation suggests that helix depth can be used to regulate membrane curvature.

As endophilin A1 is a member of a populous protein family with similar domains and functions, it is possible that the mechanisms we find here are applicable to a wide range of proteins and membrane processes. Importantly, the ability to switch between the respective structural states might be an effective means for regulating the type of membrane curvature is induced in vivo. One such regulatory mechanism could be phosphorylation. The S75 phosphorylation site is located in an aqueous environment on vesicles, whereas it is just below the phosphate level on tubes, suggesting that phosphorylation would be more destabilizing for

the latter (Fig. 3*G*). Indeed, S75D mutants decreased tube stability and enhanced vesiculation. The addition of negative charges near the C terminus of the insert region (K76E, R78E) has also been shown in previous studies to destabilize tubes (17). Thus, our data provide a structural basis for how the addition of a negative charge to amphipathic domains can act as a molecular switch to toggle between the formations of tubes and other curved structures. Because negative charges can be easily added by phosphorylation, the modification could be used to control different types of membrane curvature in vivo. Interestingly, other post-translational modification sites are located within regions found to undergo substantial movements in the present study (48). One of these sites is located in the H0 helix of endophilin A1 and has been shown to impact receptor internalization. There is also evidence of a phosphorylation site in the N termini of amphiphysin, suggesting that other BAR proteins or membrane-curving proteins may be regulated by phosphorylation. It may therefore be possible that the mechanism identified for S75 phosphorylation may be more generally applicable. The ability to regulate between tubulation and vesiculation may be important for the function of endophilin at the endocytic neck, which is transiently generated and ultimately destabilized. In fact, the inability to toggle between the phosphorylated and unphosphorylated versions of endophilin has been shown to inhibit endocytosis (4). It remains to be tested whether misregulation of this process has a direct impact in PD pathogenesis.

Materials and Methods

Detailed materials and methods are provided in *SI Materials and Methods*. Briefly, site-directed mutagenesis of the gene encoding rat endophilin A1 as well as the expression and purification of protein from *E. coli* were performed as previously described (17, 28). Proteins were spin labeled with (1-oxy-2,2,5,5-tetramethyl-d-pyrroline-3-methyl)-methanethiosulfonate and CW EPR was performed on a Bruker EMX spectrometer fitted with a dielectric resonator (17, 28). DEER measurements were made using a Bruker Elexsys E580 X-band pulse spectrometer fitted with a 3-mm split ring (MS-3) resonator as previously described (17, 28). A JEOL 1400 transmission electron microscope was used for samples negatively stained with 1% uranyl acetate (28).

ACKNOWLEDGMENTS. This work was supported by National Institutes of Health Grants GM063915 (to R.L.).

1. Rao Y, Haucke V (2011) Membrane shaping by the Bin/amphiphysin/Rvs (BAR) domain protein superfamily. *Cell Mol Life Sci* 68(24):3983–3993.
2. McMahon HT, Gallop JL (2005) Membrane curvature and mechanisms of dynamic cell membrane remodelling. *Nature* 438(7068):590–596.
3. Qualmann B, Koch D, Kessels MM (2011) Let's go bananas: Revisiting the endocytic BAR code. *EMBO J* 30(17):3501–3515.
4. Matta S, et al. (2012) LRRK2 controls an EndoA phosphorylation cycle in synaptic endocytosis. *Neuron* 75(6):1008–1021.
5. Bergmann C, et al. (2003) Oligophrenin 1 (OPHN1) gene mutation causes syndromic X-linked mental retardation with epilepsy, rostral ventricular enlargement and cerebellar hypoplasia. *Brain* 126(Pt 7):1537–1544.
6. Nicot A-S, et al. (2007) Mutations in amphiphysin 2 (BIN1) disrupt interaction with dynamin 2 and cause autosomal recessive centronuclear myopathy. *Nat Genet* 39(9):1134–1139.
7. De Camilli P, et al. (1993) The synaptic vesicle-associated protein amphiphysin is the 128-kD autoantigen of Stiff-Man syndrome with breast cancer. *J Exp Med* 178(6): 2219–2223.
8. Meinecke M, et al. (2013) Cooperative recruitment of dynamin and BIN/amphiphysin/Rvs (BAR) domain-containing proteins leads to GTP-dependent membrane scission. *J Biol Chem* 288(9):6651–6661.
9. Sundborger A, et al. (2011) An endophilin-dynamin complex promotes budding of clathrin-coated vesicles during synaptic vesicle recycling. *J Cell Sci* 124(pt 1):133–143.
10. Ringstad N, et al. (1999) Endophilin/SH3p4 is required for the transition from early to late stages in clathrin-mediated synaptic vesicle endocytosis. *Neuron* 24(1):143–154.
11. Milosevic I, et al. (2011) Recruitment of endophilin to clathrin-coated pit necks is required for efficient vesicle uncoating after fission. *Neuron* 72(4):587–601.
12. Soda K, et al. (2012) Role of dynamin, synaptojanin, and endophilin in podocyte foot processes. *J Clin Invest* 122(12):4401–4411.
13. Schuske KR, et al. (2003) Endophilin is required for synaptic vesicle endocytosis by localizing synaptojanin. *Neuron* 40(4):749–762.
14. Verstreken P, et al. (2003) Synaptojanin is recruited by endophilin to promote synaptic vesicle uncoating. *Neuron* 40(4):733–748.
15. Bai J, Hu Z, Dittman JS, Pym ECG, Kaplan JM (2010) Endophilin functions as a membrane-bending molecule and is delivered to endocytic zones by exocytosis. *Cell* 143(3): 430–441.
16. Farsad K, et al. (2001) Generation of high curvature membranes mediated by direct endophilin bilayer interactions. *J Cell Biol* 155(2):193–200.
17. Gallop JL, et al. (2006) Mechanism of endophilin N-BAR domain-mediated membrane curvature. *EMBO J* 25(12):2898–2910.
18. Masuda M, et al. (2006) Endophilin BAR domain drives membrane curvature by two newly identified structure-based mechanisms. *EMBO J* 25(12):2889–2897.
19. Ferguson SM, et al. (2009) Coordinated actions of actin and BAR proteins upstream of dynamin at endocytic clathrin-coated pits. *Dev Cell* 17(6):811–822.
20. Drin G, Antonny B (2010) Amphipathic helices and membrane curvature. *FEBS Lett* 584(9):1840–1847.
21. Stachowiak JC, et al. (2012) Membrane bending by protein-protein crowding. *Nat Cell Biol* 14(9):944–949.
22. Farsad K, De Camilli P (2003) Mechanisms of membrane deformation. *Curr Opin Cell Biol* 15(4):372–381.
23. Weissenhorn W (2005) Crystal structure of the endophilin-A1 BAR domain. *J Mol Biol* 351(3):653–661.
24. Peter BJ, et al. (2004) BAR domains as sensors of membrane curvature: the amphiphysin BAR structure. *Science* 303(5657):495–499.
25. Blood PD, Swenson RD, Voth GA (2008) Factors influencing local membrane curvature induction by N-BAR domains as revealed by molecular dynamics simulations. *Biophys J* 95(4):1866–1876.
26. Blood PD, Voth GA (2006) Direct observation of Bin/amphiphysin/Rvs (BAR) domain-induced membrane curvature by means of molecular dynamics simulations. *Proc Natl Acad Sci USA* 103(41):15068–15072.
27. Arkhipov A, Yin Y, Schulten K (2009) Membrane-bending mechanism of amphiphysin N-BAR domains. *Biophys J* 97(10):2727–2735.
28. Jao CC, et al. (2010) Roles of amphipathic helices and the bin/amphiphysin/rvs (BAR) domain of endophilin in membrane curvature generation. *J Biol Chem* 285(26): 20164–20170.
29. Bhatia VK, et al. (2009) Amphipathic motifs in BAR domains are essential for membrane curvature sensing. *EMBO J* 28(21):3303–3314.
30. Campelo F, McMahon HT, Kozlov MM (2008) The hydrophobic insertion mechanism of membrane curvature generation by proteins. *Biophys J* 95(5):2325–2339.
31. Mim C, Unger VM (2012) Membrane curvature and its generation by BAR proteins. *Trends Biochem Sci* 37(12):526–533.
32. Jao CC, Hegde BG, Chen J, Haworth IS, Langen R (2008) Structure of membrane-bound alpha-synuclein from site-directed spin labeling and computational refinement. *Proc Natl Acad Sci USA* 105(50):19666–19671.
33. Varkey J, et al. (2010) Membrane curvature induction and tubulation are common features of synucleins and apolipoproteins. *J Biol Chem* 285(42):32486–32493.
34. Mizuno N, Jao CC, Langen R, Steven AC (2010) Multiple modes of endophilin-mediated conversion of lipid vesicles into coated tubes: Implications for synaptic endocytosis. *J Biol Chem* 285(30):23351–23358.
35. Mim C, et al. (2012) Structural basis of membrane bending by the N-BAR protein endophilin. *Cell* 149(1):137–145.
36. Cui H, et al. (2013) Understanding the role of amphipathic helices in N-BAR domain driven membrane remodeling. *Biophys J* 104(2):404–411.
37. Altenbach C, Greenhalgh DA, Khorana HG, Hubbell WL (1994) A collision gradient method to determine the immersion depth of nitroxides in lipid bilayers: Application to spin-labeled mutants of bacteriorhodopsin. *Proc Natl Acad Sci USA* 91(5):1667–1671.
38. Langen R, Oh KJ, Cascio D, Hubbell WL (2000) Crystal structures of spin labeled T4 lysozyme mutants: implications for the interpretation of EPR spectra in terms of structure. *Biochemistry* 39(29):8396–8405.
39. Zhu C, Das SL, Baumgart T (2012) Nonlinear sorting, curvature generation, and crowding of endophilin N-BAR on tubular membranes. *Biophys J* 102(8):1837–1845.
40. Sorre B, et al. (2012) Nature of curvature coupling of amphiphysin with membranes depends on its bound density. *Proc Natl Acad Sci USA* 109(1):173–178.
41. Lai C-L, et al. (2012) Membrane binding and self-association of the epsin N-terminal homology domain. *J Mol Biol* 423(5):800–817.
42. Drin G, et al. (2007) A general amphipathic α-helical motif for sensing membrane curvature. *Nat Struct Mol Biol* 14(2):138–146.
43. Strandberg E, Killian JA (2003) Snorkeling of lysine side chains in transmembrane helices: How easy can it get? *FEBS Lett* 544(1-3):69–73.
44. Campelo F, Fabrikant G, McMahon HT, Kozlov MM (2010) Modeling membrane shaping by proteins: Focus on EHD2 and N-BAR domains. *FEBS Lett* 584(9):1830–1839.
45. Boucrot E, et al. (2012) Membrane fission is promoted by insertion of amphipathic helices and is restricted by crescent BAR domains. *Cell* 149(1):124–136.
46. Lee D-S, Hirashima N, Kirino Y (2000) Rapid transbilayer phospholipid redistribution associated with exocytotic release of neurotransmitters from cholinergic nerve terminals isolated from electric ray Narke japonica. *Neurosci Lett* 291(1):21–24.
47. Kato N, Nakanishi M, Hirashima N (2002) Transbilayer asymmetry of phospholipids in the plasma membrane regulates exocytotic release in mast cells. *Biochemistry* 41(25): 8068–8074.
48. Kaneko T, et al. (2005) Rho mediates endocytosis of epidermal growth factor receptor through phosphorylation of endophilin A1 by Rho-kinase. *Genes Cells* 10(10):973–987.